

PRIMARY ANALYSIS ON DISTRIBUTION CHARACTERISTICS OF PERMAFROST IN THE UPPER AREA OF THE SHULE RIVER WATERSHED, ON THE NORTHEASTERN EDGE OF THE QINGHAI-TIBETAN PLATEAU

Yu Sheng^{a}, Jing Li^a, Huijun Jin^a, Jichun Wu^a*

a. State Key Laboratory of Frozen Soil Engineering, Cold and Arid Regions Environmental and Engineering Research Institute, Chinese Academy of Sciences, Lanzhou 730000, China

Baisheng Ye^b, Jie Wang^b

b. State Key Laboratory of Cryospheric Science, State Key Laboratory of Cryospheric Science, Chinese Academy of Sciences, Lanzhou 730000, China

1. INTRODUCTION

Understanding the distribution patterns of permafrost is the basis for the construction and management of engineering projects in cold regions, and the evaluation of permafrost change/degradation and slope instabilities related with permafrost caused by the global climatic warming[1,2]. The area of high-altitude permafrost in China is about 1,732,000 km² and amounts to 80.6% of the total permafrost area of China[3]. The Qinghai-Tibetan Plateau is the largest area of high-elevation permafrost in the world [4]. To describe the distribution patterns of permafrost on the Qinghai-Tibetan Plateau, the Gauss curve proposed by Cheng (1982) worked well [5]. Later, two statistical models, which took elevation and latitude as input variables, with the mean annual ground temperatures as output variable, were developed to predict the distribution of permafrost along the Qinghai-Tibetan Highway and on the Qinghai-Tibetan Plateau[6,7].

The Qilianshan Mountains, a series of mountains extending in a southeast-northwestern extending direction, are located on the northeastern edge of the Qinghai-Tibetan Plateau. The Shule River Watershed is located in the western Qilian Mountains. The upper area (96.6°~99.0°E, 38.2°~40.0°N) of Shule River Watershed refers to that above the mountain-pass and has an area of approximately 11348.35km² (Fig.1).



Fig.1 Location of the study area

* Corresponding author: Cold and Arid Regions Environmental and Engineering Research Institute, Chinese Academy of Sciences, 320 Donggang West Road, Lanzhou, Gansu 730000, China. Tel.:+86 931 4967271. E-mail address: sheng@lzb.ac.cn

2. DATA AND METHODOLOGY

A field investigation along the valley of the Shule River was carried out at the beginning of May in 2008. It was found that the surface conditions in the study area were relatively uniform. Both the number of species and vegetation coverage are small, also the water content of soil is low. Therefore, it was thought that the development of permafrost in the area is influenced more by climatic than by ecological factors[8]. Based on empirical knowledge the lower limit of permafrost was deduced to be at a height of *c.* 3700m on the shady slopes and *c.* 3800m on the sunny slopes. Ten boreholes were drilled and thermistor probes were installed to get a further understanding of the distribution of permafrost and ground temperatures in the area. The depth of the boreholes was ranged from 8 to 15 meters, and the ground temperatures of permafrost were measured using thermistor probes.

In order to minimize the disadvantage of the small amount of boreholes, the ten boreholes were used to answer specific questions. BH₁, BH₂ and BH₃ (Boreholes No.1, No.2 and No.3) were used to determine the lower limit of permafrost. BH₄, BH₅, BH₆ and BH₇ (Boreholes No.4, No.5, No.6 and No.7) were used to analyze the impact of slope and aspect and BH₈, BH₉ and BH₁₀ (Boreholes No.8, No.9 and No.10) to evaluate the effects of different surface conditions (Fig.2).

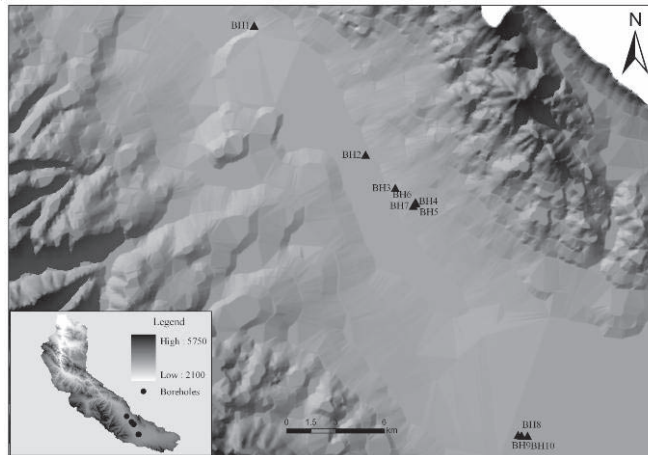


Fig.2 Sketch map of borehole locations

Locations of boreholes were recorded using a handheld Global Position System (GPS) (Garmin E-trex Summit 12XL) in WGS 84 coordinates. Elevation, slope and aspect were computed using the surface analysis procedure of the GIS software with 90m-DEM data from the Environmental and Ecological Science Data Center for West China. Effects of aspect and slope on permafrost were evaluated using the potential direct solar radiation calculated within the software of ESRI's ArcView 3.2[9,10].

On the basis of above analysis, a good linear relationship between elevation and the ground temperatures of permafrost was found and $R^2=0.9259$. According to the Gauss curve model developed by Cheng (1982) to predict the permafrost distribution of the Northern Hemisphere, effect of latitude on permafrost should not be ignored on the Qinghai-Tibetan Plateau scale and larger. The concept of equivalent-elevation was introduced and an improved linear relationship between elevation and the ground temperatures of permafrost.

In addition, the effects of aspect and slope on permafrost distribution were evaluated using the potential direct solar radiation (PDSR). Comparing ground temperatures of permafrost at the four points with the PDSRs, a significant positive correlation, and a linear relationship between the increments of PDSR and ground temperature was found. As the ground temperatures changed by 1 °C, the gradient of PDSR varied by approximately 500kWh/m²·°C.

Accordingly, a permafrost distribution model was developed.

$$GT = GT_h + \Delta GT_s$$

$$GT_h = -0.0038 * h' + 14.317 \text{ and } \Delta GT_s = (R - R_0) / 500$$

Where GT is the predicted ground temperatures of permafrost ($^{\circ}\text{C}$), $GT_{h'}$ is the ground temperature of permafrost predicted by the linear relationship between equivalent-elevation values and ground temperatures ($^{\circ}\text{C}$). ΔGT_s is the increment of ground temperature caused by aspect and slope ($^{\circ}\text{C}$), h' is the equivalent-elevation (m). R is the PDSR at a specific point (kWh/m^2) and R_0 is the benchmark value of PDSR (kWh/m^2).

The ground temperature of 0°C is the critical value of perennally frozen ground and seasonally frozen ground. According to ground temperature characteristics, permafrost is classified into low temperature ($GT \leq -2^{\circ}\text{C}$), middle temperature ($-2^{\circ}\text{C} < GT \leq -1^{\circ}\text{C}$), high temperature ($-1^{\circ}\text{C} < GT \leq -0.5^{\circ}\text{C}$) and extremely high temperature ($-0.5^{\circ}\text{C} < GT \leq 0^{\circ}\text{C}$) [11].

The model was validated by the comparing the predicted results with those of the Gauss curve, which considered only the effect of latitude on the lower limit of permafrost. The empirical correlation between lower limit of high-altitude permafrost (H) and latitude (ϕ) was as follows:

$$H = 3650 \times \exp\left[-0.003 \times (\phi - 25.37)^2\right] + 1428$$

3. RESULTS

The frozen ground map, as well as the classification map of permafrost of this area was compiled using the model within the ARCGIS software (Fig.3). The results showed that 83% or 9447.16km^2 of the upper area was underlain by perennally frozen ground. The rest area of 1901.19km^2 was underlain by the seasonally frozen ground and accounted for 17%. The main distribution of permafrost with low temperatures was at elevations 4000-5000m, and middle temperatures at 3500-4500m, and high temperatures at 2100-4500m, and extremely high temperatures at 3000-4000m.

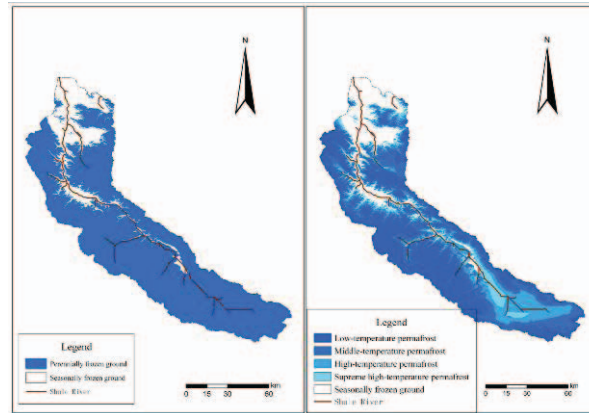


Fig.3 The permafrost distribution map of the upper area

The results of the Gauss curve showed that the distribution area of the perennally frozen ground was 9380.50km^2 corresponding to 83% and the seasonally frozen ground was 1967.85km^2 corresponding to 17%.

4. DISCUSSIONS AND CONCLUSIONS

The popular empirical-statistical models in the Alps, Scandinavia, and North America and so on, take BTS, rock glacial or ground temperatures of permafrost as the proxy of permafrost occurrence [6,7,12-16]. The basis of these kinds of models, however, is a large number of sampling points, which should cover all kinds of terrains. These methods are infeasible in the models which take ground temperatures of permafrost as dependant variables. The method used in this study is to find out the general distribution laws of permafrost and the most obvious affecting factors, and using empirical or statistical models separate the individual effect of factors. Then integrating all the single effects into one, and on this basis the distribution model of permafrost was developed. This method avoids the disadvantages of the small amounts of sampling and tried to separate the single effect of each factor. However, the work is just a start. As the work in the study area proceeds and more boreholes are

added, more local factors will be included into an improved model and more accurate distribution characteristics were analyzed.

The following conclusions were obtained.

It was feasible to evaluate the effect of latitude on permafrost through the empirical Gauss curve, and the results indicated that the effect should not be ignored even on the drainage watershed scale. The gradient of solar radiation with ground temperature of permafrost was $500\text{kWh/m}^2\cdot^\circ\text{C}$ in the study area.

The predicted area of permafrost was 9447.16km^2 which is 83% of the total area.

5. Acknowledgements

This research was supported financially by the National Basic Research Program of China (973 Program, grant no.2007CB411502), the National Innovation Fund (grant no.40821001) and the National Science Foundation of China (grant no. 40871040).

6. REFERENCES

- [1] F. Niu, G. Cheng, W. Ni, and D. Jin, "Engineering-related slope failure in permafrost regions of the Qinghai-Tibet Plateau," *Cold Regions Science and Technology*, vol.42, pp. 215-225, 2005.
- [2] Q. Wu and Y. Liu, "Ground temperature monitoring and its recent change in Qinghai-Tibet Plateau," *Cold Regions Science and Technology*, vol.38, pp. 85-92, 2004.
- [3] G. Cheng, "Problems on zonation of high-altitude permafrost," *Acta Geographica Sinica*, vol.39, no.2, pp. 185-193, 1984.
- [4] H. Jin, L. Zhao, S. Wang, and R. Jin, "The characteristics of ground temperatures and the degradation styles of permafrost along the Qinghai-Tibet highway," *Science in China (Series D)*, vol.36, pp. 1009-1019, 2006.
- [5] X. Li and G. Cheng, "The response model of high-elevation permafrost to global climate change," *Science in China (Series D)*, vol.29, pp. 185-192, 1999.
- [6] Q. Wu, X. Li, and W. Li, "Computer simulation and mapping of the regional distribution of permafrost along the Qinghai-Xizang Highway.," *Journal of Glaciology and Geocryology*, vol.22, pp. 323-326, 2000.
- [7] Z. Nan, S. Li, and Y. Liu, "Mean annual ground temperature distribution on the Tibetan Plateau permafrost distribution mapping and further application," *Journal of Glaciology and Geocryology*, vol.24, pp. 142-148, 2002.
- [8] J. Wu, Y. Sheng, J. Li, and J Wang, "Permafrost in Source Areas of Shule River in Qilian Mountains," *Acta Geographica Sinica*, vol.64, no.5, pp. 571-580, 2009.
- [9] E.S.F. Heggem, B. Etzelmüller, and I. Berthling, "Topographic radiation balance models:sensitivity and application in periglacial geomorphology," *Norwegian Journal of Geography*, vol.55, pp. 203-211, 2001.
- [10] P. Fu and P.M. Rich, "Design and implementation of the Solar Analyst: an ArcView extension for modeling solar radiation at landscape scales", 2004.
- [11] Z. Wu, Y. Liu, "Frozen Subsoil and Engineering". Beijing: Ocean Press, 2005.
- [12] S. Gruber and M. Hoelzle, "Statistical modelling of mountain permafrost distribution--local calibration and incorporation of remotely sensed data," *Permafrost and Periglacial Processes*, vol.12, pp. 69-77, 2001.
- [13] A.G. Lewkowicz and M. Ednie, "Probability Mapping of Mountain Permafrost Using the BTS Method, Wolf Creek, Yukon Territory, Canada.," *Permafrost and Periglacial Processes*, vol.15, pp. 67-80, 2004.
- [14] E.S.F. Heggem, H. Juliussen, B. Etzelmüller, "Mountain permafrost in Central-Eastern Norway," *Norwegian Journal of Geography*, vol.59, no.2, pp.94-108, 2005.
- [15] A. Julián and J. Chueca, "Permafrost distribution from BTS measurements (Sierra de Telera, Central Pyrenees, Spain): assessing the importance of solar radiation in a mid-elevation shaded mountainous area," *Permafrost and Periglacial Processes*, vol.18, pp. 137-149, 2007.
- [16] J.R. Janke, "The occurrence of alpine permafrost in the Front Range of Colorado," *Geomorphology*, vol.67, no.3, pp. 375-389, 2005.